Interpretation of acceptor excitation spectra in uniaxially stressed germanium

J. Broeckx* and J. Vennik
Laboratorium voor Kristallografie en Studie van de Vaste Stof, Rijksuniversiteit Gent, Krijgslaan 281/S1, B9000 Gent, Belgium
(Received 10 October 1986)

The irreducible-spherical-tensor method of Baldereschi and Lipari is extended to include the effect of uniaxial stress on the energy levels of effective-mass acceptors in cubic semiconductors. The Hamiltonians with uniaxial stress along ⟨001⟩ and ⟨111⟩ are developed explicitly. The method is then applied to acceptors in germanium. The binding energies of the ground state and the first 18 odd-parity excited states with uniaxial stress along each of both directions are computed for stress intensities ranging from 10^6 to 10^9 Pa. This covers the low-, intermediate-, and high-stress regions. The results are compared to the available experimental data from far-infrared piezospectroscopy, and the calculation is found to be very accurate up to the high-stress limit.

INTRODUCTION

Accurate numerical solutions to the acceptor problem in effective-mass theory (EMT)[1] have only been obtained during the past 10 yr by Baldereschi and Lipari,[2,3] who have reformulated the EMT acceptor Hamiltonian in irreducible-spherical-tensor form. In this paper we present an extension of that method to the case where uniaxial stress is present along a ⟨001⟩ or a ⟨111⟩ direction. We will give a brief description of our method, which we will then apply to acceptors in uniaxially stressed germanium. A more thorough discussion of the method and of the results for Ge and Si will be published elsewhere.

THEORY

When no external perturbations are present, the EMT acceptor Hamiltonian is a 6×6 matrix, which can be written as the sum of the Kohn-Luttinger acceptor Hamiltonian without spin[1] and a spin-orbit interaction matrix,[2,3]

$$-\tfrac{2}{3}(\tfrac{1}{2}-\mathbf{I}\cdot\mathbf{S})\Delta_0 .$$

The components of $\mathbf{I}$ and $\mathbf{S}$ are the angular momentum matrices for spin 1 and for spin $\frac{1}{2}$, respectively. Total angular momentum of a hole in the valence band is $\mathbf{J}=\mathbf{I}+\mathbf{S}$, and Δ_0 is the spin-orbit splitting energy between the $\Gamma_8^+(J=\frac{3}{2})$ and $\Gamma_7^+(J=\frac{1}{2})$ band edges. Baldereschi and Lipari[4] have introduced the parameters

$$\mu=\frac{6\gamma_3+4\gamma_2}{5\gamma_1},\quad \delta=\frac{\gamma_3-\gamma_2}{\gamma_1},$$

where $\gamma_1,\gamma_2,\gamma_3$ are the Kohn-Luttinger valence-band parameters.[1] Using the components of $\mathbf{I}$ and of $\mathbf{p}=-i\hbar\nabla$, they have defined also the second-rank Cartesian tensor operators

$$P_{ij}=\frac{1}{\hbar^2}(3p_ip_j-\delta_{ij}p^2),$$

$$I_{ij}=\tfrac{3}{2}(I_iI_j+I_jI_i)-\delta_{ij}I^2,$$

which are symmetric and have vanishing trace, and therefore decompose into the components of irreducible-spherical-tensor operators[5] $P^{(2)}$ and $I^{(2)}$ of rank 2 only. The zero-stress EMT acceptor Hamiltonian according to Baldereschi and Lipari is[2,3]

$$H_{\rm acc}^{\rm T=0}=-\frac{p^2}{\hbar^2}+\frac{\epsilon_\infty}{\epsilon(r)}\frac{2}{r}-\tfrac{2}{3}(\tfrac{1}{2}-\mathbf{I}\cdot\mathbf{S})\Delta_0+\tfrac{1}{3}\mu(P^{(2)}\circ I^{(2)})-\tfrac{1}{3}\delta\left[[P^{(2)}\times I^{(2)}]^{(4)}_{-4}+\frac{\sqrt{70}}{5}[P^{(2)}\times I^{(2)}]^{(4)}_{0}+[P^{(2)}\times I^{(2)}]^{(4)}_{+4}\right]. \tag{1}$$

A point-charge potential with diagonal q-dependent dielectric screening had been used; the zero for the energy scale lies at the Γ_8^+ band edge, and energy and length are expressed in units of the effective Rydberg R_0^* and the effective Bohr radius a_0^*, defined as

$$R_0^*=\frac{1}{(4\pi\epsilon_0)^2}\frac{m_0e^4}{2\hbar^2\gamma_1\epsilon_\infty},\quad a_0^*=4\pi\epsilon_0\frac{\hbar^2\gamma_1\epsilon_\infty}{m_0e^2},$$

with ϵ_∞ the static dielectric constant, and $\Delta_0^*=\Delta_0/R_0^*$. The x,y,z axes in (1) coincide with the *cubic crystal axes*.

When uniaxial stress is applied, the stress interaction matrix has to be added to the EMT acceptor Hamiltonian. In the same coordinate system, and to lowest order in the strain tensor ϵ_{ij}, it is[6]

$$H_{\rm stress}=D_d^*(\epsilon_{xx}+\epsilon_{yy}+\epsilon_{zz})+2D_u^*[(I_x^2-\tfrac{1}{3}I^2)\epsilon_{xx}+\text{c.p.}]+4D_u^{*\prime}[\{I_yI_z\}\epsilon_{yz}+\text{c.p.}], \tag{2}$$

where c.p. denotes cyclic permutation of the indices x,y,z, and $\{ab\}=\frac{1}{2}(ab+ba)$. The scalars $D_d^*, D_u^*, D_u^{*'}$ are the Kleiner-Roth deformation potentials[7] expressed in units of R_0^*. The term in D_d^*, associated with the dilatation component, simply shifts the entire valence-band multiplet without splitting it. It will be dropped from now on, because it is of no relevance whatsoever for the acceptor problem.

A uniform stress parallel to $\langle 001\rangle$ is represented in the coordinate system in use by the following strain tensor:

$$\epsilon_{xx}=\epsilon_{yy}=-s_{12}T;\quad \epsilon_{zz}=-s_{11}T;\quad \epsilon_{yz}=\epsilon_{zx}=\epsilon_{xy}=0\ .$$

The cubic compliance constants are denoted by s_{11}, s_{12}, and s_{44}. T is the stress intensity, defined to be positive for compression. After substitution into (2) and reduction to irreducible-spherical-tensor components, we obtain our final expression

$$H_{\rm acc}^{\overline{T}||111}=-\frac{p^2}{\hbar^2}+\frac{\epsilon_\infty}{\epsilon(r)}\frac{2}{r}-\tfrac{2}{3}(\tfrac{1}{2}-\mathbf{I}\cdot\mathbf{S})\Delta_0^*+\tfrac{1}{3}\mu(P^{(2)}\circ I^{(2)})$$
$$+\tfrac{2}{9}\delta\left[2[P^{(2)}\times I^2]^{(4)}_{-3}+\frac{\sqrt{70}}{5}[P^{(2)}\times I^{(2)}]^{(4)}_0-2[P^{(2)}\times I^{(2)}]^{(4)}_{+3}\right]+(\tfrac{2}{3})^{3/2}D_u^{*'}(\tfrac{1}{2}s_{44})I_0^{(2)}T\ . \quad (4)$$

The z axis of the coordinate system for this Hamiltonian lies along one of the threefold symmetry axes of the lattice; its symmetry group is $\overline{D}_{3d}$.

The EMT equation with $H_{\rm acc}^{\mathbf{T}||\langle 001\rangle}$ or $H_{\rm acc}^{\mathbf{T}||\langle 111\rangle}$ has been solved variationally. The eigenfunctions for a given row ρ of a given irreducible representation Γ_R of $\overline{D}_{4h}$ or $\overline{D}_{3d}$ are expanded into an orthogonal series of angular basis functions belonging to Γ_R^ρ, multiplied by unknown radial functions. The angular basis functions are constructed as linear combinations with different F_z of the angular momentum eigenfunctions $|L,(I,S)J,F,F_z\rangle$ in the L-J—coupled scheme. $\mathbf{L}$ is the angular momentum associated with the space coordinates (θ,ϕ), and $\mathbf{F}=\mathbf{L}+\mathbf{J}$. The series has been truncated by the criterion $L\leq 7$, which guaranteed good convergence of the energies. The number of basis functions was then between 42 and 72. The angular matrix elements were evaluated numerically by the computer program using the reduced matrix element technique,[5] and the resulting set of radial differential equations was solved variationally by the expansion of each radial function into a number of exponentials with fixed exponents, multiplied by a power of r.

RESULTS

Computed binding energies for the two ground state components with uniaxial stress parallel to $\langle 001\rangle$ and to $\langle 111\rangle$ are shown in Fig. 1. Throughout the low stress region, up to 2×10^8 Pa, the *splitting* is linear, as expected from deformation-potential theory, but the entire ground-state multiplet experiences a quadratic upward shift. We found, with E in meV and T in Pa,

$$H_{\rm stress}^{\mathbf{T}||\langle 001\rangle}=(\tfrac{2}{3})^{3/2}D_u^*(s_{11}-s_{12})I_0^{(2)}T\ , \quad (3)$$

which is to be added to (1) to form our EMT acceptor Hamiltonian $H_{\rm acc}^{\mathbf{T}||\langle 001\rangle}$ with stress parallel to $\langle 001\rangle$, having $\overline{D}_{4h}$ symmetry.

A uniform stress parallel to $\langle 111\rangle$ is represented in the same coordinate system by the strain tensor

$$\epsilon_{xx}=\epsilon_{yy}=\epsilon_{zz}=-\tfrac{1}{3}(s_{11}+2s_{12})T\ ;$$
$$\epsilon_{yz}=\epsilon_{zx}=\epsilon_{xy}=-\tfrac{1}{6}s_{44}T\ .$$

Substitution into (2) and reduction to spherical components gives a complicated expression containing different $I_q^{(2)}$. The expression simplifies if we rotate the coordinate system over the Eulerian angles $\alpha=+\pi/4$, $\beta=\arccos(1/\sqrt{3})$, $\gamma=0$, in order to make the quantization axis coincide with the stress direction:

$$\mathbf{T}||\langle 001\rangle:\ E=\pm 0.1345\times 10^{-7}T+1.98\times 10^{-17}T^2\ ,$$
$$\mathbf{T}||\langle 111\rangle:\ E=\pm 0.1121\times 10^{-7}T+0.90\times 10^{-17}T^2\ ,$$

which gives for the ground-state deformation potentials,

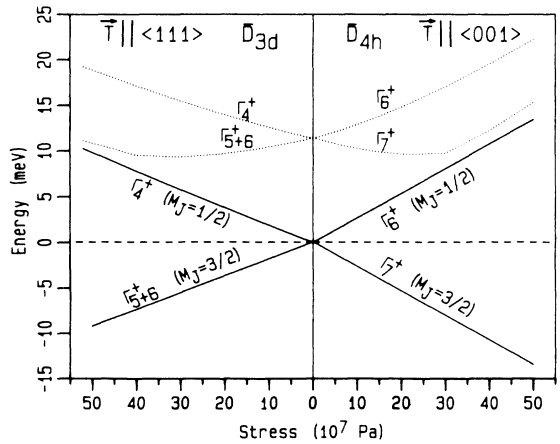

FIG. 1. Computed energies of the stress-split acceptor ground state compared to the splitting of the Γ_8^+ valence band edge, for uniaxial stress parallel to $\langle 001\rangle$ and to $\langle 111\rangle$. Valence band parameters, deformation potentials, and cubic compliance constants used throughout our calculation are [J.C. Hensel and K. Suzuki, Phys. Rev. B **9**, 4219 (1974)], $\gamma_1=13.38$, $\gamma_2=4.24$, $\gamma_3=5.69$, $\Delta_0=0.290$ eV, $D_u=3.32$ eV, $D_u'=3.81$ eV; $s_{11}=9.55\times 10^{-12}$ Pa^{-1}, $s_{12}=-2.62\times 10^{-12}$ Pa^{-1}, $s_{44}=14.58\times 10^{-12}$ Pa^{-1}. The dielectric function $\epsilon_\infty/\epsilon(r)$ is derived from the $\epsilon(q)$ given by Richardson and Vinsome [D. Richardson and P. K. W. Vinsome, Phys. Lett. **36A**, 3 (1971)], adjusted to $\epsilon_\infty=15.36$ for Ge at low temperatures [R. A. Faulkner, Phys. Rev. **184**, 713 (1969)].

$$D_{GS}/D_u = 0.499, \quad D'_{GS}/D'_u = 0.605 .$$

With increasing stress, the energies no longer follow a simple power law in the stress intensity due to interactions with even parity excited states of the same symmetry. Kinks may even occur in the curves, which result from "anticrossings."

Figures 2 and 3 show the computed binding energies as a function of the stress intensity for the odd-parity excited states involved in the G, D, B, A_4, A_3, A_2, and A_1 lines observed by far-infrared spectroscopy.[8] At very low stress, the splittings of the $G^*(1\Gamma_8^-)$, $D^*(2\Gamma_8^-)$, and $B^*(4\Gamma_8^-)$ levels are linear, but quadratic shifts are present here too. Interactions between states of like symmetry dominate the energy spectrum in the intermediate-stress region, leading to a complicated pattern involving many anticrossings, which cannot possibly be inferred from a perturbation calculation starting with the zero-stress wave functions. In the high-stress region ($T \geq 5\times 10^8$ Pa) the energy spectrum simplifies again, because the valence bands effectively decouple. As we discussed it in a previously written paper,[9] the EMT equation which applies in the high-stress limit derives from an oblate ellipsoid band edge, giving the level identifications shown at the right in the figures.

In Figs. 4–6 a comparison is made between our computed transition energies for electric-dipole transitions originating in the ground-state multiplet, and the experimental line positions from far-infrared piezo spectroscopy[10–12] corrected for the *zero-stress chemical shift*. We

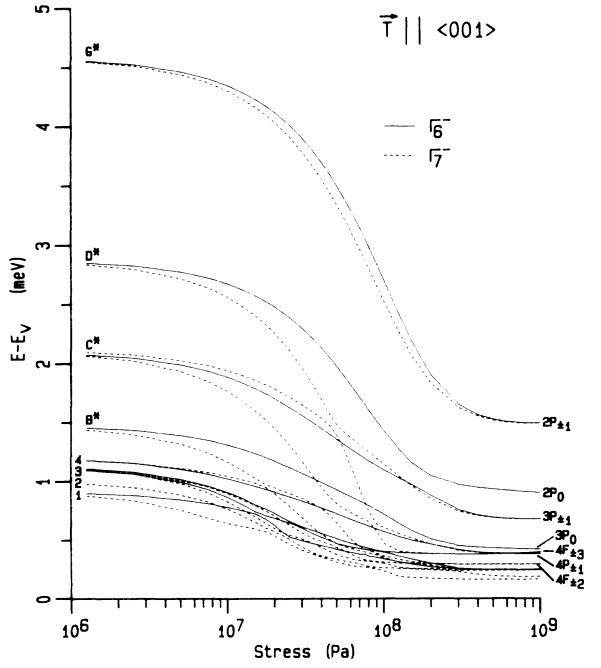

FIG. 2. Stress dependence of the computed binding energies for the first 18 odd-parity excited states with uniaxial stress along ⟨001⟩. The zero for the energy scale lies at the $\Gamma_6^+(M_J=\pm\frac{1}{2})$ band edge. Labeling on the left-hand side corresponds to the zero-stress spectrum, and that on the right-hand side to the high-stress limit.

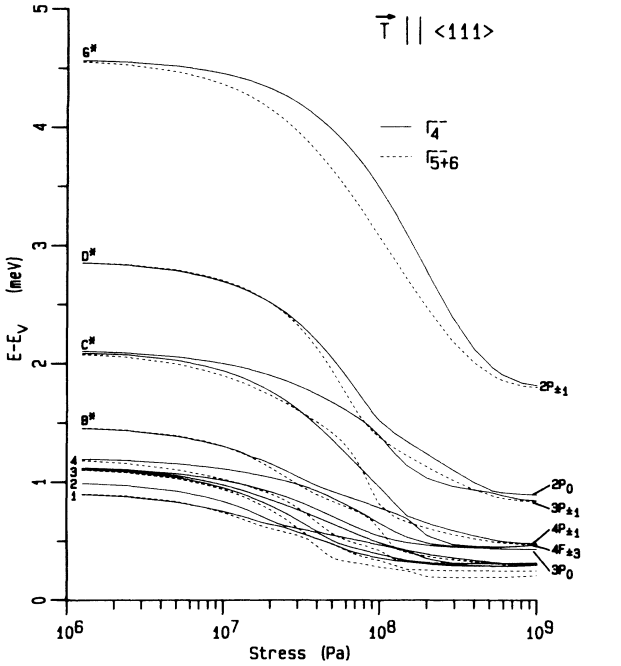

FIG. 3. Same as Fig. 2 but with uniaxial stress along ⟨111⟩. The zero for the energy scale lies at the $\Gamma_4^+(M_J=\pm\frac{1}{2})$ band edge.

determined this chemical shift for a given acceptor impurity as the difference between the experimental zero-stress D-line position and the computed energy separation between $1\Gamma_8^+(O_h)$ and $2\Gamma_8^-(O_h)$. Assuming the chemical shift to be stress independent, we added it to all the experimental line positions with stress, in order to be able to

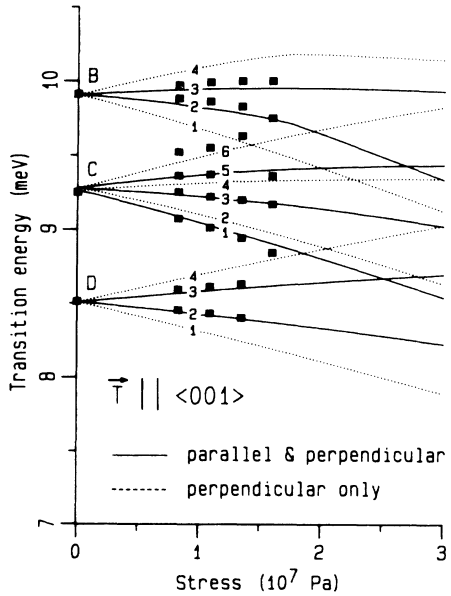

FIG. 4. Comparison between the computed transition energies in the low-stress region for uniaxial stress along ⟨001⟩, and the experimental data for the In acceptor from Ref. 10. Experimental line positions have been corrected for the chemical shift as explained in the text.

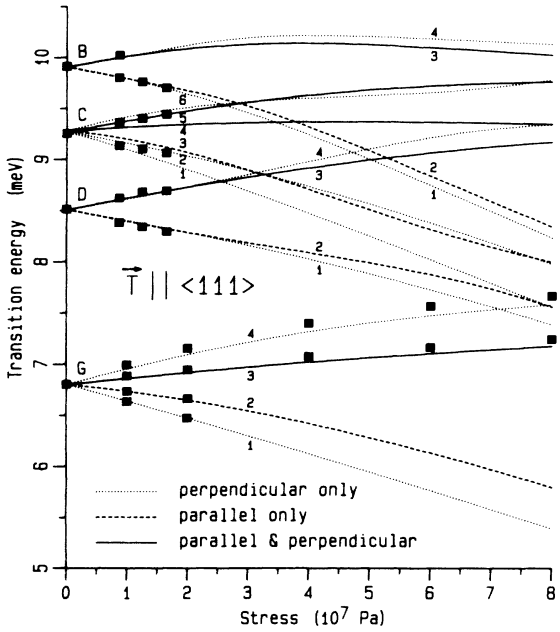

FIG. 5. Comparison between the computed transition energies in the low- to intermediate-stress region for uniaxial stress along ⟨111⟩, and the experimental data for the D, C, and B lines of In from Ref. 10 and the G line of Ga from Ref. 11. Corrections for the chemical shift have been applied as explained in the text.

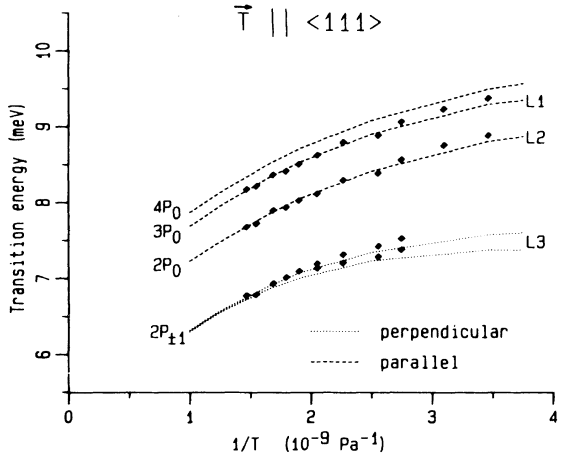

FIG. 6. Predictions for the observable transitions in the high-stress limit with uniaxial stress along ⟨111⟩, compared to the experimental data for Al from Ref. 12, corrected for the chemical shift.

compare them with the theoretical predictions. From Figs. 4 and 5 it is clear that the comparison shows an almost perfect agreement in the low to intermediate stress region. There are, however, several symmetry allowed transitions which are not observed experimentally. We have computed the oscillator strengths for all the electric-dipole allowed transitions. Full details will be published elsewhere, but we found that the unobserved lines have very small oscillator strengths indeed. As an example, in the D multiplet at $T=10^7$ Pa and parallel to ⟨001⟩ the computed oscillator strengths in the perpendicular polarization have the ratios $D_1{:}D_2{:}D_3{:}D_4 = 9{:}112{:}52{:}9$, which explains the absence of D_1 and D_4 in the spectra.

The most amazing result from our calculation, however, is shown in Fig. 6. It gives a comparison of our predictions for the line positions of the first five acceptor transitions with non-negligible oscillator strengths in the *high-stress limit,* to the experimental observations for the Al acceptor.[12] Again the *zero-stress chemical shift* has been added to the data. The identification of the final states follows the notation for the high-stress limit, but the agreement with experiment is many times better than what follows from our previous calculation based on the EMT equation for that limit.[9] This means that the decoupling of the valence bands is still far from complete. It demonstrates also the great accuracy which can be attained with our new method, even in the high-stress limit.

We wish to acknowledge useful discussions with Dr. A. Baldereschi concerning an early version of his acceptor program for octahedral symmetry, and we would like to thank Dr. P. Clauws for his constant support of our work.

*Present address: Université du Burundi, Faculté des Sciences, BP 2700, Bujumbura, République du Burundi.

[1]J. M. Luttinger and W. Kohn, Phys. Rev. **97**, 869 (1955).

[2]A. Baldereschi and N. O. Lipari, *Proceedings of the 13th International Conference on Physics of Semiconductors, Roma, 1976,* edited by F. G. Fumi (North-Holland, Amsterdam, 1976), p. 595.

[3]N. O. Lipari and A. Baldereschi, Solid State Commun. **25**, 665 (1978).

[4]A. Baldereschi and N. O. Lipari, Phys. Rev. B **8**, 2697 (1973).

[5]A. R. Edmonds, *Angular Momentum in Quantum Mechanics* (Princeton University Press, Princeton, 1974).

[6]H. Hasegawa, Phys. Rev. **129**, 1029 (1963).

[7]W. H. Kleiner and L. M. Roth, Phys. Rev. Lett. **2**, 334 (1959). The deformation potentials used by G. L. Bir, E. I. Butikov, and G. E. Picus, J. Phys. Chem. Solids **24**, 1467 (1963) are related to the Kleiner-Roth parameters through the following: $a=+D_d$, $b=-\frac{2}{3}D_u$, $d=-(2/\sqrt{3})D_u'$.

[8]The present notation for the A lines has been introduced by E. E. Haller and W. L. Hansen, Solid State Commun. **15**, 687 (1974).

[9]J. Broeckx, P. Clauws, and J. Vennik, J. Phys. C **19**, 511 (1986).

[10]D. H. Dickey and J. O. Dimmock, J. Phys. Chem. Solids **28**, 529 (1967).

[11]A. D. Martin, P. Fisher, C. A. Freeth, E. H. Salib, and P. E. Simmonds, Phys. Lett. **99A**, 391 (1983).

[12]A. G. Kazanskii, P. L. Richards, and E. E. Haller, Solid State Commun. **24**, 603 (1977).